

# Sterile neutrino production in models with low reheating temperatures

---

**Carlos E. Yaguna**

*Department of Physics and Astronomy, UCLA, 475 Portola Plaza, Los Angeles, CA 90095, USA*

*E-mail:* yaguna@physics.ucla.edu

**ABSTRACT:** By numerically solving the appropriate Boltzmann equations, we study the production of sterile neutrinos in models with low reheating temperatures. We take into account the production in oscillations as well as in direct decays and compute the sterile neutrino primordial spectrum, the effective number of neutrino species, and the sterile neutrino contribution to the mass density of the Universe as a function of the mixing and the reheating parameters. It is shown that sterile neutrinos with non-negligible mixing angles do not necessarily lead to  $N_\nu \sim 4$  and that sterile neutrinos may have the right relic density to explain the dark matter of the Universe. If dark matter consists of sterile neutrinos produced in oscillations, X-rays measurements set a strong limit on the reheating temperature,  $T_R \gtrsim 7$  MeV. We also point out that the direct decay opens up a new production mechanism for sterile neutrino dark matter where cosmological constraints can be satisfied.

**KEYWORDS:** neutrinos, cosmology, dark matter.

---

## Contents

<b>1. Introduction</b>	<b>1</b>
<b>2. The reheating process</b>	<b>3</b>
<b>3. Active neutrinos and low <math>T_R</math></b>	<b>6</b>
<b>4. Sterile neutrino production in oscillations</b>	<b>8</b>
<b>5. Sterile neutrino production in oscillations and decays</b>	<b>12</b>
<b>6. Conclusions</b>	<b>14</b>

---

## 1. Introduction

Sterile neutrinos likely exist. They can easily be incorporated into the standard model and provide the simplest explanation for the existence of neutrino masses. The most important parameter associated with sterile neutrinos is probably their mass scale. In seesaw models [1], where sterile neutrinos are simply added to the standard model matter fields in order to generate light neutrino masses, sterile neutrino masses are free parameters of the Lagrangian, whose values are to be experimentally determined. To account for the neutrino masses inferred from the solar and atmospheric neutrino experiments, at least two sterile neutrinos are required but only mild constraints on the masses or mixing of the sterile neutrinos can be derived. And theoretical considerations are of no help either, for heavy as well as light sterile neutrinos can be motivated on different grounds [2, 3]. It seems reasonable, then, to consider the sterile neutrino mass scale simply as another free parameter subject to present experimental constraints. In this paper, we study sterile neutrinos with masses in the eV–keV range.

Sterile neutrinos with keV masses have indeed been proposed as dark matter candidates [4, 5, 6]. In the early Universe, such sterile neutrinos are produced in active-sterile neutrino oscillations and never reach thermal equilibrium. Due to their primordial velocity distribution, sterile neutrinos damp inhomogeneities on small scales and therefore behave as warm dark matter particles. The mass of dark matter sterile neutrinos is constrained from below by the observed clustering on small scales of the Lyman- $\alpha$  forest [7]. Present bounds give  $m_s > 10\text{--}14$  keV [8, 9]. Because of its mixing with active neutrinos, the  $\nu_s$  may radiatively decay (through  $\nu_s \rightarrow \nu + \gamma$ ) producing a monoenergetic photon with  $E_\gamma \sim m_s/2$ . X-rays

measurements may therefore be used to constraint or infer the mass of the sterile neutrino. Recent bounds, based on observations of the Virgo and Coma clusters and the X-ray background, yield  $m_s < 6\text{--}10$  keV [10, 11, 12] and are thus in conflict with the Lyman- $\alpha$  forest constraint. That means that the minimal mechanism for sterile neutrino dark matter, based on active-sterile oscillations, is already ruled out [10, 8, 9].

A possible clue regarding the mass scale of the sterile neutrinos is the result of the LSND experiment [13]. It found evidence of  $\bar{\nu}_\mu \rightarrow \bar{\nu}_e$  conversion, which is being tested by the Fermilab MiniBoone experiment [14]. The LSND signal can be explained by the existence of light ( $m_s \sim 1\text{--}10$  eV) sterile neutrinos mixed with  $\nu_e$  and  $\nu_\mu$  [2]. In the standard cosmological model, such sterile neutrinos generate two important problems: i) They give a contribution to  $\Omega_\nu$  larger than that suggested by global fits of CMD and LSS data [15]. ii) They thermalize in the early Universe so that  $N_\nu \sim 4$ , in possible conflict with big-bang nucleosynthesis bounds [16]. Recently, the MiniBoone experiment presented its first results [17] which disfavore even more the so-called (3+1) schemes [18]. It seems, nonetheless, that (3+2) schemes are still viable [18].

The standard cosmological model, however, has not been tested beyond big bang nucleosynthesis, for  $T \gtrsim 1$  MeV. Cosmological models with low reheating temperatures, for example, offer a natural and viable alternative to the standard paradigm. In fact, various scenarios of physics beyond the standard model, including supersymmetry and superstring theories, predict the existence of massive particles with long lifetimes that decay about the big bang nucleosynthesis epoch, inducing a low reheating temperature and modifying the initial conditions of the standard cosmology. Over the years, different issues related to these models have been studied in the literature [19, 20, 21]. In this paper we consider the possible interplay between sterile neutrinos and models with low reheating temperatures. On the one hand, sterile neutrinos may serve as probes of the early Universe and constrain the reheating temperature. On the other hand, models with low reheating temperatures may alleviate some of the problems associated with sterile neutrinos, suppressing their abundance or modifying the standard relation between the sterile neutrino relic density and the mixing parameters.

So far, a detailed analysis of these effects have not been presented in the literature. Cosmologies with low reheating temperatures were suggested, in [16], as a possible way to accommodate the LSND signal and big bang nucleosynthesis, whereas in [22], several simplifying assumptions -not all of them justified- were used to obtain an analytic estimation of the sterile neutrinos produced in oscillations. In this paper, we numerically solve the equations that determine the sterile neutrino distribution function in models with low reheating temperatures. Two different sources of sterile neutrinos are taken into account: active-sterile oscillations and the direct decay of the field responsible for the reheating process. We compute different observables related to the sterile neutrino, including its spectrum and relic density, as a function of the reheating parameters and the mixing angle and mass of the sterile neutrino.

In the next section we describe the reheating process and introduce the different equations that are relevant for the production of sterile neutrinos. Then, the behavior of active neutrinos in models with low reheating temperatures will be briefly reviewed. In section 4, we study

in detail the production of sterile neutrinos as a result of active-sterile neutrino oscillations for different mixing and reheating parameters. We show that  $N_\nu \sim 3$  can be obtained even for sterile neutrinos with relatively large mixing angles and that dark matter sterile neutrinos provide a strong constraint on the reheating temperature. Finally, in section 5, we include the production of sterile neutrinos through the direct decay of the scalar field and study the resulting sterile neutrino spectrum and relic density. We observe that sterile neutrinos produced in decays may account for the dark matter and avoid the Lyman- $\alpha$  and X-ray constraints.

## 2. The reheating process

Reheating is defined as the transition period between a Universe dominated by a unstable non-relativistic particle,  $\phi$ , and the radiation dominated Universe. In the standard cosmological model reheating is assumed to occur only after inflation, but in general, additional reheating phases not related to inflation are also possible and our discussion applies equally to them. During reheating the dynamics of the Universe is rather involved. The energy density per comoving volume of the non-relativistic particle decreases as  $e^{-\Gamma_\phi t}$  -with  $\Gamma_\phi$  the  $\phi$  decay width- whereas the light decay products of the  $\phi$  field thermalize. Their temperature quickly reaches a maximum value  $T_{max}$  and then decreases as  $T \propto a^{-3/8}$  [20], as a result of the continuous entropy release. During this time the relation between the expansion rate and the temperature is neither that of a matter-dominated universe ( $H \propto T^{3/2}$ ) nor that of a radiation-dominated Universe ( $H \propto T^4$ ) but it is given instead by  $H \propto T^4$ . Thus, at a given temperature the Universe expands faster during reheating than in the radiation-dominated era. This unusual behavior continues until  $t \sim \Gamma_\phi^{-1}$ , when the radiation dominated phase commences with temperature  $T_R$ . From then on, that is for  $T < T_R$ , the evolution of the Universe proceeds as in the standard scenario but with initial conditions determined by the reheating process.

The success of standard big bang nucleosynthesis provides the strongest constraint on  $T_R$ . Electrons and photons interact electromagnetically and consequently have large creation, annihilation and scattering rates that keep them in equilibrium even during reheating. Neutrinos, on the contrary, can interact only through the weak interactions and are slowly produced in electron-positron annihilations. Since big bang nucleosynthesis requires a thermal neutrino spectrum,  $T_R$  should be high enough to allow the thermalization of the neutrino sea. Given that, in the standard cosmology, neutrinos decouple from the thermal plasma at  $T \sim 2 - 3$  MeV, it can be estimated that they will not thermalize if  $T_R < \text{few MeV}$ . Indeed, detailed calculations give  $T \gtrsim 2 - 4$  MeV [19, 21] as the present bound. In this paper, we consider models with reheating temperatures below 10 MeV.

Let us now formulate the equations that describe the reheating process, and in particular, the production of sterile neutrinos at low reheating temperatures. We denote by  $\phi$  the unstable non-relativistic particle that initially dominates the energy density of the Universe.

Its energy density,  $\rho_\phi$ , evolves according to

$$\frac{d\rho_\phi}{dt} = -\Gamma_\phi \rho_\phi - 3H\rho_\phi \quad (2.1)$$

where  $H$  is the Hubble parameter and  $\Gamma_\phi$  is the  $\phi$  decay width.

The energy-momentum conservation equation in the expanding universe is

$$\frac{d\rho_T}{dt} = -3H(\rho_T + P_T) \quad (2.2)$$

where  $\rho_T$  and  $P_T$  denote respectively the total energy density and the total pressure. At the low temperatures we allow for, only the scalar field, electrons, photons, and neutrinos are present in the plasma. Denoting by  $\rho_\nu$  the energy density in active and sterile neutrinos, we have that

$$\rho_T(t) = \rho_\phi + \rho_\gamma + \rho_e + \rho_\nu \quad (2.3)$$

and an analogous expression holds for  $P_T$ . Equation (2.2) can be rewritten as an evolution equation for the (photon) temperature as

$$\frac{dT_\gamma}{dt} = -\frac{-\rho_\phi \Gamma_\phi + 4H\rho_\gamma + 3H(\rho_e + P_e) + 4H\rho_\nu + d\rho_\nu/dt}{\partial\rho_\gamma/\partial T_\gamma + \partial\rho_e/\partial T_\gamma}. \quad (2.4)$$

$H$ , the hubble parameter, is given by the Friedmann equation,

$$H(t) = \frac{\dot{a}(t)}{a(t)} = \sqrt{\frac{8\pi}{3} \frac{\rho_T}{M_P^2}} \quad (2.5)$$

with  $a$  the scale factor and  $M_P$  the Planck mass .

We follow the evolution of active neutrinos by solving the momentum-dependent Boltzmann equation

$$\frac{\partial f_\nu}{\partial t} - Hp \frac{\partial f_\nu}{\partial p} = C_{coll} \quad (2.6)$$

for  $\nu_e$  and  $\nu_\mu$  ( $f_{\nu_\tau} = f_{\nu_\mu}$ ).  $C_{coll}$ , the total collision term, describes neutrino annihilations and scatterings. The following processes are taken into account in our calculations:

$$\nu_i + \nu_i \leftrightarrow e^+ + e^- \quad (2.7)$$

$$\nu_i + e^\pm \leftrightarrow \nu_i + e^\pm. \quad (2.8)$$

The collision terms associated with these processes are complicated, involving nine-dimensional integrations over momentum space. But they can be simplified to one-dimensional integrals by neglecting  $m_e$  and assuming that electrons obey the Boltzmann distribution [19]. Since the error due to the above approximations is small (less than few percent), we will use the one-dimensional form of the collision terms.

Regarding the sterile neutrinos, we will consider the simplifying limit of two neutrino (active-sterile) mixing. That is, we assume one sterile neutrino,  $\nu_s$ , that mixes predominantly

with a single active flavor  $\nu_\alpha$  ( $\alpha = e, \mu, \tau$ ). In consequence, the transformation between the flavor and the mass bases can be written as

$$|\nu_\alpha\rangle = \cos\theta |\nu_1\rangle + \sin\theta |\nu_2\rangle \quad (2.9)$$

$$|\nu_s\rangle = -\sin\theta |\nu_1\rangle + \cos\theta |\nu_2\rangle \quad (2.10)$$

where  $|\nu_1\rangle$  and  $|\nu_2\rangle$  are neutrino mass eigenstates with masses  $m_1$  and  $m_2$ , respectively.  $\theta$ , the mixing angle, parameterizes the magnitude of the mixing between the active and the sterile neutrino. For the small mixing angles we deal with,  $|\nu_2\rangle$  practically coincides with  $|\nu_s\rangle$ , so we will use  $m_s$  instead of  $m_2$  to denote the mass of the eigenstate that is predominantly sterile.

The sterile neutrino distribution function also follows a Boltzmann equation like (2.6). The collision term for  $\nu_\alpha \leftrightarrow \nu_s$  oscillations is [5]:

$$C_{\nu_s \leftrightarrow \nu_\alpha} = \frac{1}{4} \frac{\Gamma_\alpha(p) \Delta^2(p) \sin^2 2\theta}{\Delta^2(p) \sin^2 2\theta + D^2(p) + [\Delta(p) \cos 2\theta - V^T(p)]^2} [f_\alpha(p, t) - f_s(p, t)] \quad (2.11)$$

where  $\Delta(p) = m_s^2/2p$ ,  $\Gamma_\alpha$  is the  $\nu_\alpha$  total interaction rate,  $D(p) = \Gamma_\alpha/2$  is the quantum damping rate, and  $V^T$  is the thermal potential.

In addition to oscillations, we also consider the production of sterile neutrinos through the direct decay  $\phi \rightarrow \nu_s \nu_s$ . Since  $\phi$  is nonrelativistic, each sterile neutrino is born with momentum  $m_\phi/2$  and the collision integral becomes

$$C_{\phi \rightarrow \nu_s \nu_s} = b \frac{2\pi^2}{(m_\phi/2)^2} \Gamma_\phi n_\phi \delta(p - m_\phi/2), \quad (2.12)$$

where  $b$  is the branching ratio into sterile neutrinos, and  $m_\phi, n_\phi$  are respectively the  $\phi$  mass and number density.

As initial conditions we assume that at early times the energy-density of the Universe is dominated by  $\phi$ , and that active and sterile neutrinos are absent from the primordial plasma. As long as the maximum temperature reached by the plasma ( $T_{max}$  [20]) is large enough, the final outcome is independent of the initial conditions. We found that  $T_{max} \sim 20$  MeV is enough to guarantee such independence.

Our analysis can naturally be divided into two parts: production in oscillations only ( $b = 0$ ), and production in oscillations and decay ( $b \neq 0$ ). In the first case, to be investigated in section 4, the parameters that enter into the above equations are  $m_s$ ,  $\sin^2 2\theta$ , and  $\Gamma_\phi$ . It is customary to trade  $\Gamma_\phi$  with the cosmological parameter  $T_R$  -known as the reheating temperature- through the relations

$$\Gamma_\phi = 3H(T_R) \quad (2.13)$$

and

$$H(T_R) = 3 \frac{T_R^2}{M_P} \left( \frac{8\pi^3 g_*}{90} \right)^{1/2}. \quad (2.14)$$

with  $g_* = 10.75$ . These equations establish a one-to-one correspondence between  $\Gamma_\phi$  and  $T_R$ . In the second case, when sterile neutrinos are also produced in decays ( $b \neq 0$ ), the results will depend additionally on  $b$  and  $m_\phi$ . Section 5 deals with this interesting possibility.

For a given set of mixing and reheating parameters, we simultaneously follow the evolution of  $\rho_\phi$ ,  $T_\gamma$ ,  $f_{\nu_e}(p)$ ,  $f_{\nu_\mu}(p)$ , and  $f_{\nu_s}(p)$  from the matter dominated era well into the radiation-dominated Universe, until the distribution functions reach their asymptotic values ( $T < 0.1$  MeV). The main output from this system of equations are the neutrino distribution functions, which can be used to compute several observables. Big bang nucleosynthesis, for instance, is sensitive to the relativistic energy density in neutrinos. This quantity is usually parameterized in units of the energy density of a standard model neutrino,  $\rho_{\nu_0}$ , and denoted by  $N_\nu$ ,

$$N_\nu = \frac{\rho_{\nu_e} + \rho_{\nu_\mu} + \rho_{\nu_\tau} + \rho_{\nu_s}}{\rho_{\nu_0}}. \quad (2.15)$$

Since sterile neutrinos are dark matter candidates, it is also important to compute their relic abundance,

$$\Omega_s = \frac{m_s n_s}{\rho_c}, \quad (2.16)$$

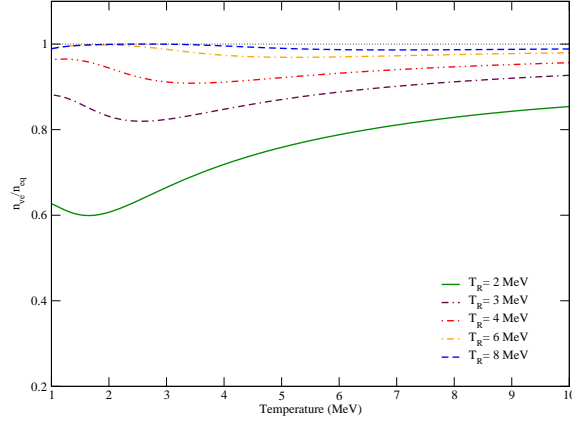
where  $m_s, n_s$  are respectively the mass and number density of the sterile neutrinos, and  $\rho_c$  is the critical density of the Universe.

### 3. Active neutrinos and low $T_R$

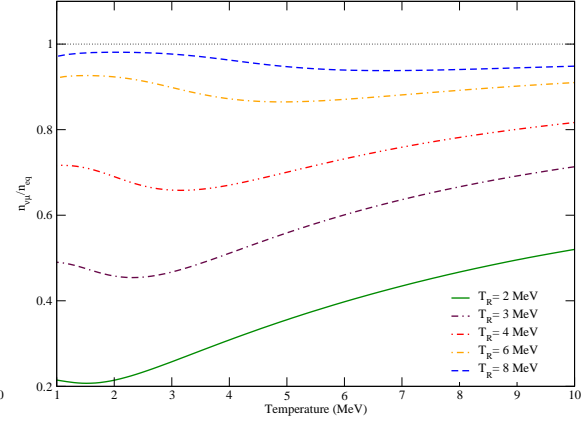
The evolution of the sterile neutrino distribution function strongly depends on the corresponding function of the active neutrino flavor with which it mixes and it is in many ways analogous to it. Before considering sterile neutrinos, it is therefore appropriate to briefly review the salient features related to the behavior of active neutrinos in models with low reheating temperatures.

Figure 1 shows the evolution of the electron neutrino number density (normalized to the equilibrium density) as a function of the temperature for different reheating temperatures. The pattern is clear. At high temperatures,  $T \gg T_R$ , neutrinos are out of equilibrium and  $n_{\nu_e}/n_{eq}$  continually decreases with time until  $T \sim T_R$  is reached. For  $T < T_R$ , neutrinos evolve as in the radiation dominated but with a non-equilibrium initial condition ( $n_{\nu_e}(T_R) \neq n_{eq}(T_R)$ ). If  $T_R$  is large enough, neutrinos will be able to recover the equilibrium distribution before decoupling from the thermal plasma. Such event, illustrated by the line  $T_R = 8$  MeV in figure 1, would be indistinguishable from the standard cosmology. For smaller reheating temperatures, on the other hand, neutrinos never reach the equilibrium distribution and decouple from the plasma with a smaller abundance than in the standard scenario. That is exactly what happens, for instance, if  $T_R \lesssim 4$  MeV (see figure 1). Note nonetheless that even for  $T_R = 3$  MeV the asymptotic deviation from the standard prediction amounts to less than 10%.

Because muons are not present in the thermal plasma at low temperatures, muon neutrinos can only be produced in neutral-current interactions. Consequently, the muon neutrino



**Figure 1:** The evolution of the electron neutrino number density as a function of the photon temperature for different reheating temperatures.



**Figure 2:** The evolution of the muon (or tau) neutrino number density as a function of the photon temperature for different reheating temperatures.

deviates from equilibrium farther than the electron neutrino, as revealed in figure 2. Indeed, for  $T_R = 3$  MeV the deviation from the standard prediction amounts to 50%.

The effects of the reheating process can also be seen in the primordial neutrino spectrum. A equilibrium spectrum with  $T_\nu = T_\gamma/1.4$  is expected in the standard cosmological model. Figure 3 shows the  $\nu_\mu$  primordial energy spectrum for different values of  $T_R$  as a function of  $p/T_\gamma$ . The deviation from equilibrium is clearly visible for the smaller reheating temperatures.

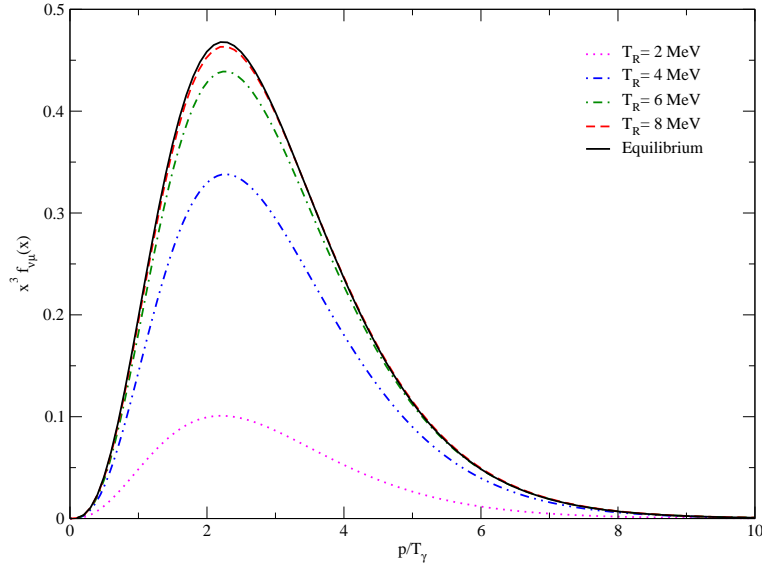


**Figure 3:** The primordial energy spectrum of the muon neutrino as a function of  $p/T_\gamma$  for different reheating temperatures.



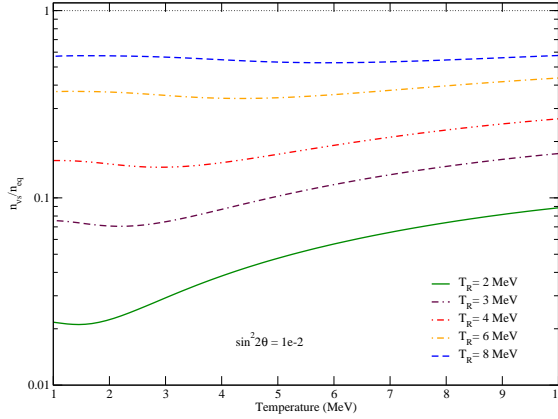


**Figure 4:** The evolution of the sterile neutrino number density as a function of the photon temperature for different reheating temperatures and  $\sin^2 2\theta = 10^{-2}$ .

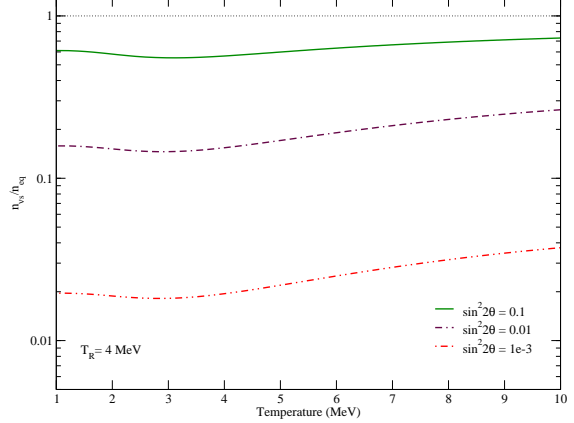


**Figure 5:** The evolution of the sterile neutrino number density as a function of the photon temperature for different mixing angles and  $T_R = 4$  MeV.

#### 4. Sterile neutrino production in oscillations

Let us now consider the production of sterile neutrinos through active-sterile neutrino oscillations. For simplicity we will consider mixing with the electron neutrino only so that  $\sin^2 2\theta$  denotes the mixing angle between  $\nu_e$  and  $\nu_s$ . We are then left with 3 parameters that determine all the observables:  $T_R$ ,  $\sin^2 2\theta$ , and  $m_s$ . In this section we study how these parameters affect  $f_{\nu_s}$ ,  $N_\nu$ , and  $\Omega_{\nu_s}$ .

The evolution of the sterile neutrino number density follows a pattern similar to that of the active neutrinos. Figure 5 shows  $n_{\nu_s}/n_{eq}$  as a function of the temperature for different values of  $T_R$  and  $\sin^2 2\theta = 10^{-2}$ . Sterile neutrinos are always out of equilibrium and  $n_{\nu_s}/n_{eq}$  decreases with time during the reheating phase, reaching its minimum value at  $T \sim T_R$ . At  $T \lesssim T_R$ , the universe is radiation dominated and the sterile neutrino population slightly increases, in part as a result of the corresponding increase in  $n_{\nu_e}$  (see figure 1). The asymptotic value of  $n_{\nu_s}/n_{eq}$ , however, differs very little from its value at  $T_R$ .

Note that this result is at odds with [22], where it was *assumed* that the production of sterile neutrinos starts at  $T_R$ . Actually, as we have seen, sterile neutrinos are slowly created during the  $\phi$  dominated era and only a small fraction of them are produced after  $T_R$ .

For the range of sterile neutrino masses considered,  $n_{\nu_s}/n_{eq}$  does not depend on  $m_s$ . Thus, the other relevant dependence to investigate is that with  $\sin^2 2\theta$ . In figure 4,  $n_{\nu_s}/n_{eq}$  is shown as a function of the temperature for  $T_R = 4$  MeV and different mixing angles. As expected, the smaller the mixing angle the smaller  $n_{\nu_s}/n_{eq}$ . Indeed, for small mixing angles ( $\sin^2 2\theta \lesssim 10^{-2}$ ),  $n_{\nu_s}/n_{eq} \propto \sin^2 2\theta$ , as seen in figure 4. Such proportionality is expected when  $f_{\nu_s}$  can be neglected with respect to  $f_{\nu_e}$  in equation (2.11). At large mixing angles  $f_{\nu_s}$  may become comparable with  $f_{\nu_e}$  and the above relation no longer holds. Neglecting  $f_{\nu_s}$  in (2.11), therefore, is not a good approximation for sterile neutrinos with large mixing angles.

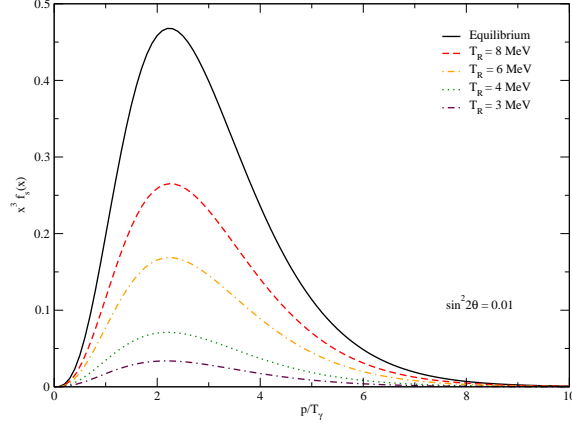


**Figure 6:** The primordial energy spectrum of the sterile neutrino as a function of  $p/T_\gamma$  for different reheating temperatures and  $\sin^2 2\theta = 10^{-2}$ .

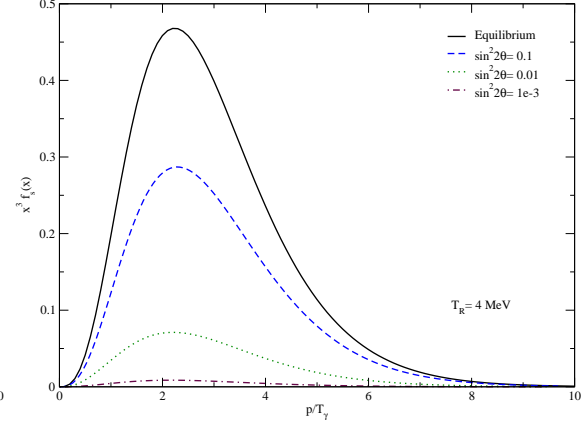


**Figure 7:** The primordial energy spectrum of the sterile neutrino as a function of  $p/T_\gamma$  for different mixing angles and  $T_R = 4$  MeV.

The primordial energy spectrum of the sterile neutrino is shown in figures 6 and 7 for different values of  $T_R$  and  $\sin^2 2\theta$ . It is certainly non-thermal and is strongly suppressed for low reheating temperatures or small mixing angles.

Standard big bang nucleosynthesis is a powerful cosmological probe of active and sterile neutrino effects. It constrains the number of thermalized neutrinos present at  $T \sim 0.1-1$  MeV to be  $N_\nu = 2.5 \pm 0.7$  [23]. Unfortunately, the uncertainty in  $N_\nu$  is controversial so not strict bound on it can be derived. Here, we will simply take as a reference value the prediction of

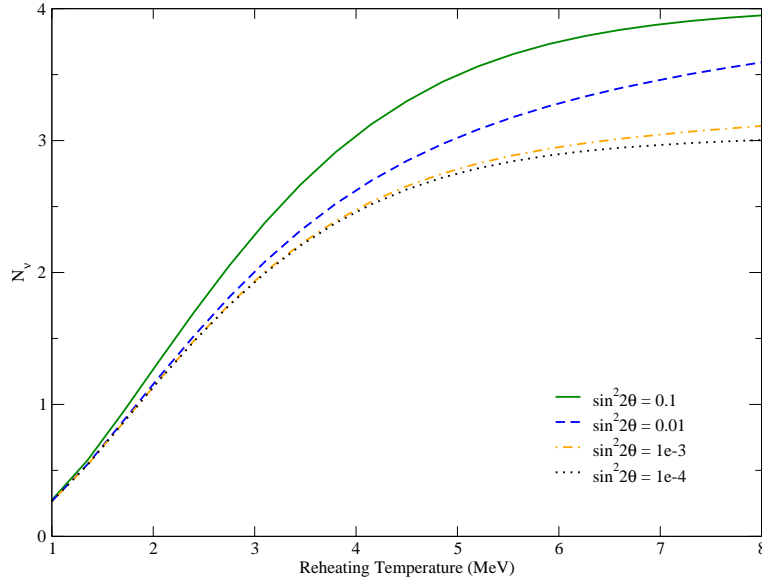


**Figure 8:** The effective number of neutrino species as a function of  $T_R$  for different mixing angles.

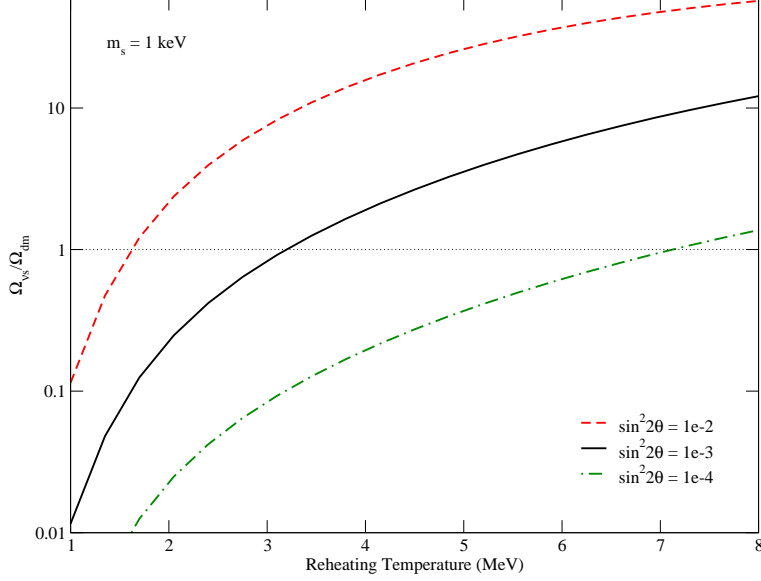


**Figure 9:**  $\Omega_{\nu_s}/\Omega_{dm}$  as a function of  $T_R$  for different mixing angles and  $m_s = 1$  keV.

the standard cosmological model,  $N_\nu = 3$ . Figure 8 shows  $N_\nu$  as a function of  $T_R$  for different mixing angles. The variation with  $T_R$  is strong, going from  $N_\nu \sim 3 - 4$  for  $T_R \gtrsim 7$  MeV to  $N_\nu \sim 0.3$  for  $T_R = 1$  MeV. The spread due to different mixing angles, on the other hand, is maximum ( $\Delta N_\nu \sim 1$ ) at large  $T_R$ , and decreases for smaller  $T_R$ . Note that for  $\sin^2 2\theta \lesssim 10^{-3}$ ,  $N_\nu$  is essentially insensitive to the presence of sterile neutrinos; it becomes a function only of  $T_R$ . As expected, the standard cosmological scenario is recovered at large  $T_R$ . In that region, if the mixing angle is large  $\sin^2 2\theta \sim 0.1$  all neutrinos -the three active plus the sterile- thermalize, yielding  $N_\nu \sim 4$ . That is not necessarily the case for lower reheating temperatures, however. If  $T_R \sim 4$  MeV, for instance, then  $N_\nu \sim 3$  for a sterile neutrino with  $\sin^2 2\theta \sim 0.1$ ; and the same  $N_\nu$  can be obtained for  $\sin^2 2\theta \sim 10^{-2}$  and  $T_R = 5$  MeV. Hence, LSND sterile neutrinos may still yield  $N_\nu \sim 3$ , avoiding possible conflicts with big bang nucleosynthesis.

The sterile neutrino relic density as a function of  $T_R$  is shown in figure 9 for different mixing angles and  $m_s = 1$  keV. Along the horizontal line, sterile neutrinos entirely account for the dark matter density of the Universe. The region above the horizontal line is therefore ruled out, whereas below it,  $\nu_s$  only partially contribute to the dark matter density. Thus, in the region  $3 \text{ MeV} < T_R < 7 \text{ MeV}$  and  $10^{-3} > \sin^2 2\theta > 10^{-4}$  a sterile neutrino with  $m_s = 1$  keV may explain the dark matter.

Because  $\Omega_{\nu_s}$  scales linearly with  $m_s$ , the results for a different value of  $m_s$  can easily be obtained from the same figure. First notice from the figure that the sterile neutrino relic density also depends linearly on  $\sin^2 2\theta$ . So, another region where  $\Omega_{\nu_s} = \Omega_{dm}$  is  $m_s = 10$  keV,  $3 \text{ MeV} < T_R < 7 \text{ MeV}$  and  $10^{-4} > \sin^2 2\theta > 10^{-5}$ .

In the standard cosmological scenario, dark matter sterile neutrinos are produced at  $T \sim 150$  MeV where collisions dominate the evolution of the neutrino system and matter

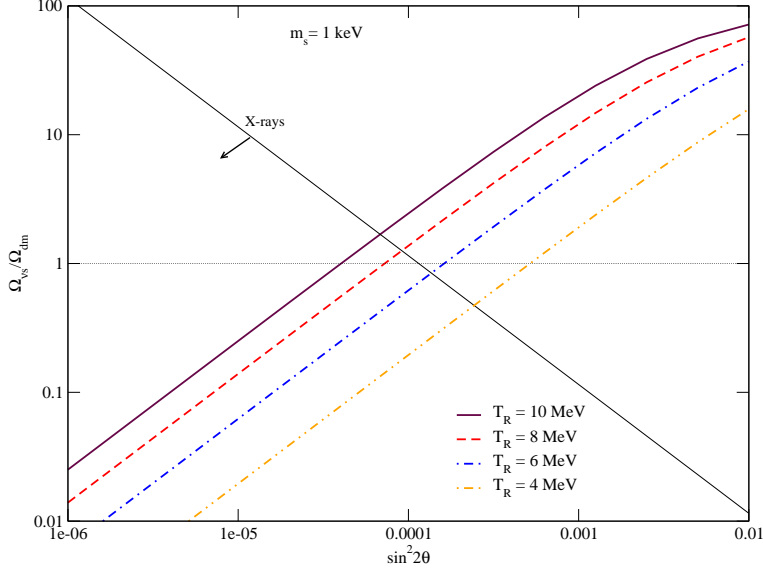


**Figure 10:** The sterile neutrino relic density as a function of  $\sin^2 2\theta$ .

and thermal effects become relevant. As a result, the sterile neutrino relic density depends quadratically on  $m_s$  and keV sterile neutrinos with  $\sin^2 2\theta \sim 10^{-8}$  are required to account for the dark matter. In models with low reheating temperature, on the other hand,  $\Omega_{\nu_s}$  depends linearly on  $m_s$  and much larger mixing angles are required to explain the dark matter.

Cosmological and astrophysical observations can be used to constrain sterile neutrinos as dark matter candidates. The observed clustering on small scales of the Lyman- $\alpha$  forest, for instance, constrains the sterile neutrino mass from below. To obtain a limit on  $m_s$ , the flux power spectrum of the Lyman- $\alpha$  forest must be carefully modeled using numerical simulations. The analysis presented in [8] and [9] respectively cite  $m_s > 10$  keV and  $m_s > 14$  keV as their limits, though a 30% discrepancy between them still exists. Such bounds, however, were obtained for sterile neutrinos produced in the standard cosmological model and do not directly apply to the scenario we consider. That is why we will be mainly concerned with another bound, that derived from X-rays measurements. Sterile neutrinos may radiatively decay through  $\nu_s \rightarrow \nu_\alpha + \gamma$  producing a monoenergetic photon,  $E_\gamma = m_s/2$ . X-ray observations may therefore be used to constrain or infer the mass of the sterile neutrino. In a recent analysis of the X-ray background from HEAO-1 and XMM-Newton, for example, the following limit

$$\sin^2 2\theta < 1.15 \times 10^{-4} \left( \frac{m_s}{\text{keV}} \right)^{-5} \left( \frac{0.26}{\Omega_{\nu_s}} \right) \quad (4.1)$$

relating  $\sin^2 2\theta$ ,  $m_s$  and  $\Omega_{\nu_s}$  was found [11]. This bound is model independent, it applies to both the standard production mechanism and to the production in models with low reheating temperatures.

In figure 10 we display the sterile neutrino relic density as a function of  $\sin^2 2\theta$  for different values of  $T_R$  and  $m_s = 1$  keV. The limit from X-rays, equation (4.1), is also shown and

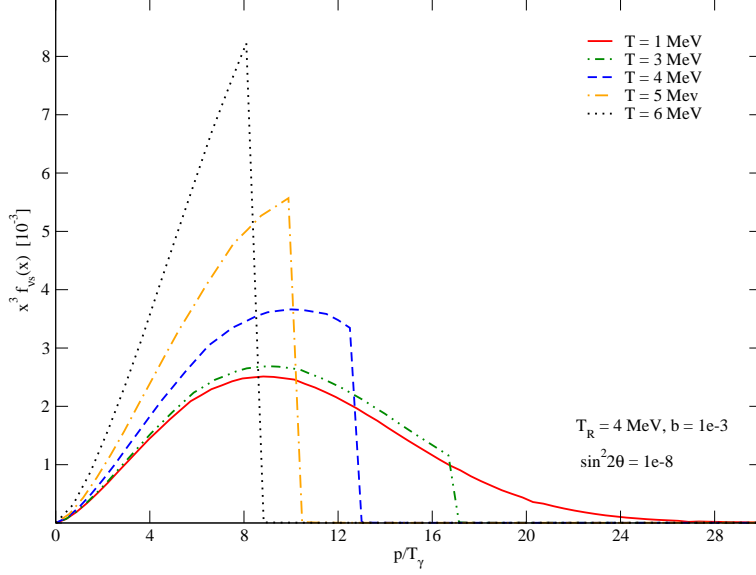


**Figure 11:** The evolution of the sterile neutrino energy spectrum for  $T_R = 4$  MeV,  $b = 10^{-3}$  and  $\sin^2 2\theta = 10^{-8}$ .

rules out the upper-right part of the figure. The different lines represent different reheating temperatures. Notice, for instance, that  $T_R = 4$  MeV,  $\Omega_{\nu_s} = \Omega_{dm}$  is not a viable point of the parameter space as it is incompatible with the X-rays limit. Indeed, sterile neutrinos can account for the dark matter only if  $T_R \gtrsim 7$  MeV.

Turning this argument around we can also say that if dark matter consists of sterile neutrinos, they provide the strongest constraint on the reheating temperature. The present bound, in fact, gives  $T_R \gtrsim 2 - 4$  MeV and is based on the effect of active neutrinos on big bang nucleosynthesis. Dark matter sterile neutrinos might yield a more stringent constraint. Finally, notice that this bound on  $T_R$  was obtained for a sterile neutrino with  $m_s = 1$  keV but it only becomes stronger for larger masses. Dark matter sterile neutrinos, therefore, are useful probes of the early Universe.

## 5. Sterile neutrino production in oscillations and decays

The field  $\phi$  responsible for the reheating process may also have a direct decay mode into sterile neutrinos ( $\phi \rightarrow \nu_s \nu_s$ ), opening an additional production mechanism for  $\nu_s$ . As we will see, this mechanism significantly alters the predictions obtained in the previous section. In [25], the production of sterile neutrinos in inflaton decays was investigated, but not in the context of low reheating temperatures. The main motivation to consider this mechanism is the conflict between the constraints from X-ray observations and those from small-scale structure that rule out the minimal production scenario for sterile neutrino dark matter.

As mentioned in section 2, the decay  $\phi \rightarrow \nu_s \nu_s$  gives the following contribution to the

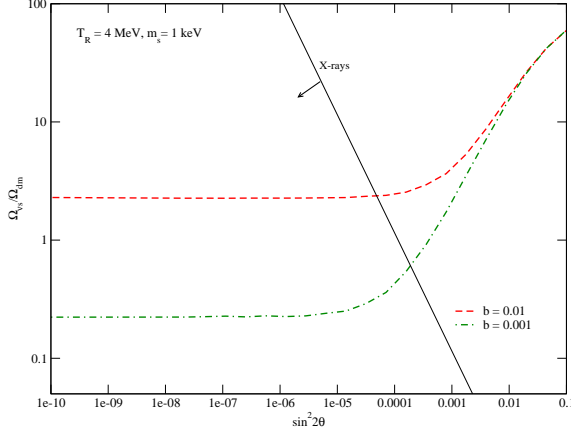


**Figure 12:** The sterile neutrino relic density as a function of  $\sin^2 2\theta$  for  $T_R = 4$  MeV. The sterile neutrino mass is set to 1 keV and the curves correspond to two different values of  $b$ . The bound from X-rays observations is also shown.

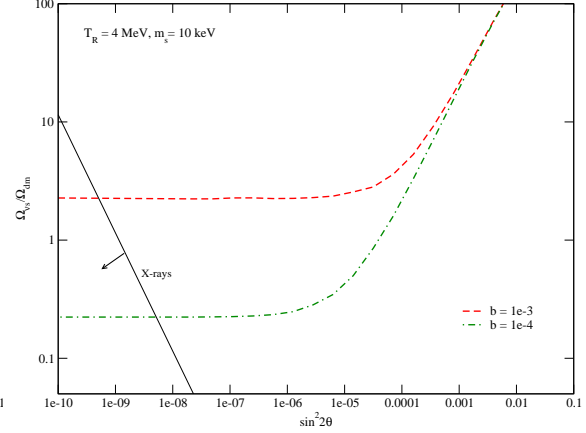


**Figure 13:** The sterile neutrino relic density as a function of  $\sin^2 2\theta$  for  $T_R = 4$  MeV. The sterile neutrino mass is set to 10 keV and the curves correspond to two different values of  $b$ . The bound from X-rays observations is also shown.

sterile neutrino collision integral

$$C_{\phi \rightarrow \nu_s \nu_s} = b \frac{2\pi^2}{(m_\phi/2)^2} \Gamma_\phi n_\phi \delta(p - m_\phi/2), \quad (5.1)$$

where  $b$  denotes the  $\phi$  branching ratio into sterile neutrinos, and  $m_\phi$ ,  $n_\phi$  are respectively the  $\phi$  mass and number density. Being  $\phi$  non-relativistic, each  $\nu_s$  is born with momentum  $p = m_\phi/2$ , as enforced by the delta function. Due to this new contribution,  $f_{\nu_s}$  will now depend not only on  $T_R$ ,  $m_s$ , and  $\sin^2 2\theta$  but also on  $b$  and  $m_\phi$ . To keep things simple we will set  $m_\phi = 100$  MeV and study the dependence of the different observables with  $b$ .

Figure 11 displays the evolution of the sterile neutrino energy spectrum for  $T_R = 4$  MeV,  $b = 10^{-3}$ , and  $\sin^2 2\theta = 10^{-8}$ . Each line corresponds to a different temperature. It is not difficult to decipher what is going on. Whenever a  $\phi$  decays, a peak at  $p = m_\phi/2$  in  $f_{\nu_s}$  is generated. But not all  $\phi$ 's decay at the same time. And the momentum of the sterile neutrinos produced in earlier decays is redshifted when later decays occur. That is why, at any given temperature, the resulting spectrum has a drastic jump at  $p \sim m_\phi/2$ , with all the neutrinos produced before (in decays) lying at smaller momenta. As we approach the radiation dominated epoch, the redshift essentially ceases and only residual decays modify the spectrum at large  $p/T_\gamma$ . At the end, no traces of the discontinuity at  $p = m_\phi/2$  are left in the primordial spectrum.

The sterile neutrino relic density is shown in figure 12 as a function of  $\sin^2 2\theta$ . For that figure  $T_R = 4$  MeV,  $m_s = 1$  keV and the two curves correspond to  $b = 10^{-2}$  and  $b = 10^{-3}$ . The solid line is the X-ray constraint obtained from equation (4.1). The relic density behaves in a similar way for the different values of  $b$ . At large mixing angles, the production of sterile

neutrinos is dominated by oscillations and independent of  $b$ . That is the case we dealt with in the previous section. At smaller mixing angles, we encounter an intermediate region where both production mechanisms are relevant and the relic density depends on  $b$  and  $\sin^2 2\theta$ . Finally, at even smaller mixing angles, sterile neutrinos are produced dominantly in  $\phi$  decays and therefore the relic density does not depend on  $\sin^2 2\theta$ , as signaled by the horizontal lines observed in figure 12. In that region the sterile neutrino relic density is simply proportional to  $b$ . If sterile neutrinos account for the dark matter,  $\Omega_{\nu_s} = \Omega_{dm}$ , the X-rays constraint requires a small mixing angle,  $\sin^2 2\theta \lesssim 10^{-4}$ .

New viable regions, where the sterile neutrino is produced in  $\phi$  decays and makes up the dark matter of the Universe, can be read off figures 12 and 13. For instance, a  $m_s = 1$  keV sterile neutrino with  $\sin^2 2\theta < 10^{-4}$  will be a good dark matter candidate for  $T_R \sim 4$  MeV and  $10^{-3} < b < 10^{-2}$ . For decay-dominated production,  $\Omega_{\nu_s}$  is simply proportional to  $T_R$ ,

$$\Omega_{\nu_s} \propto b m_s T_R. \quad (5.2)$$

Using this equation in conjunction with figures 12 and 13, additional allowed regions can be found.

Figure 13 is analogous to figure 12 but for a larger value of the sterile neutrino mass,  $m_s = 10$  keV. The two curves correspond to  $b = 10^{-3}$  and  $b = 10^{-4}$ . Owing to the increase in  $m_s$ , the X-ray limit becomes much stronger than in figure 12. Indeed, it constrains dark matter sterile neutrinos to have a very small mixing angle,  $\sin^2 2\theta \lesssim 10^{-9}$ .

In the standard production mechanism, such small mixing angles are not allowed as they yield a too small sterile neutrino relic density,  $\Omega_{\nu_s} \propto \sin^2 2\theta$ . For sterile neutrinos originating in  $\phi$  decays, on the contrary, the production mechanism and the radiative decay are controlled by two different parameters. In fact,  $\Omega_{\nu_s} \propto b$  whereas  $\Gamma(\nu_s \rightarrow \nu_\alpha + \gamma) \propto \sin^2 2\theta$ . Thus, no matter how small  $\sin^2 2\theta$  -and consequently  $\Gamma(\nu_s \rightarrow \nu_\alpha + \gamma)$ - is, it is still possible to find appropriate values of  $b$ ,  $T_R$  and  $m_s$  such that  $\Omega_{\nu_s} = \Omega_{dm}$ . In other words, for  $b \neq 0$  the X-rays limit can always be satisfied.

## 6. Conclusions

We numerically studied the production of sterile neutrinos in models with low reheating temperatures. Two production mechanisms for the sterile neutrinos were taken into account: active-sterile neutrino oscillations ( $\nu_\alpha \leftrightarrow \nu_s$ ) and the direct decay of the scalar field ( $\phi \rightarrow \nu_s \nu_s$ ). Several observables, including  $f_{\nu_s}$ ,  $N_\nu$ , and  $\Omega_{\nu_s}$ , were computed for different sets of reheating and mixing parameters. We showed that in these models, LSND sterile neutrinos may still give  $N_\nu \sim 3$  –avoiding problems with big bang nucleosynthesis– and that keV sterile neutrinos may account for the dark matter of the Universe. Dark matter sterile neutrinos produced in oscillations were found to be effective probes of the early Universe, as they constrain the reheating temperature to be rather large,  $T_R \gtrsim 7$  MeV. Finally, we showed that sterile neutrinos originating in decays may explain the dark matter and satisfy the bounds from X-ray observations.

## Acknowledgments

I would like to thank A. Kusenko and G. Gelmini for their comments and useful suggestions.

## References

- [1] P. Minkowski, Phys. Lett. B **67**, 421 (1977). R. N. Mohapatra and G. Senjanovic, Phys. Rev. Lett. **44**, 912 (1980).
- [2] A. de Gouvea, Phys. Rev. D **72**, 033005 (2005) [arXiv:hep-ph/0501039].
- [3] A. Kusenko, arXiv:hep-ph/0703116.
- [4] S. Dodelson and L. M. Widrow, Phys. Rev. Lett. **72**, 17 (1994) [arXiv:hep-ph/9303287].
- [5] K. Abazajian, G. M. Fuller and M. Patel, Phys. Rev. D **64**, 023501 (2001) [arXiv:astro-ph/0101524].
- [6] A. D. Dolgov and S. H. Hansen, Astropart. Phys. **16**, 339 (2002) [arXiv:hep-ph/0009083].  
X. D. Shi and G. M. Fuller, Phys. Rev. Lett. **82**, 2832 (1999) [arXiv:astro-ph/9810076].
- [7] S. H. Hansen, J. Lesgourgues, S. Pastor and J. Silk, Mon. Not. Roy. Astron. Soc. **333**, 544 (2002) [arXiv:astro-ph/0106108].
- [8] U. Seljak, A. Makarov, P. McDonald and H. Trac, Phys. Rev. Lett. **97**, 191303 (2006) [arXiv:astro-ph/0602430].
- [9] M. Viel, J. Lesgourgues, M. G. Haehnelt, S. Matarrese and A. Riotto, Phys. Rev. Lett. **97**, 071301 (2006) [arXiv:astro-ph/0605706].
- [10] K. Abazajian and S. M. Koushiappas, Phys. Rev. D **74**, 023527 (2006) [arXiv:astro-ph/0605271].
- [11] A. Boyarsky, A. Neronov, O. Ruchayskiy and M. Shaposhnikov, Mon. Not. Roy. Astron. Soc. **370**, 213 (2006) [arXiv:astro-ph/0512509].
- [12] A. Boyarsky, A. Neronov, O. Ruchayskiy and M. Shaposhnikov, Phys. Rev. D **74**, 103506 (2006) [arXiv:astro-ph/0603368].
- [13] C. Athanassopoulos *et al.* [LSND Collaboration], Phys. Rev. Lett. **77**, 3082 (1996) [arXiv:nucl-ex/9605003].  
C. Athanassopoulos *et al.* [LSND Collaboration], Phys. Rev. C **58**, 2489 (1998) [arXiv:nucl-ex/9706006].  
C. Athanassopoulos *et al.* [LSND Collaboration], Phys. Rev. Lett. **81**, 1774 (1998) [arXiv:nucl-ex/9709006].
- [14] I. Stancu [MiniBooNE Collaboration], Nucl. Phys. Proc. Suppl. **155**, 164 (2006).
- [15] A. Pierce and H. Murayama, Phys. Lett. B **581**, 218 (2004) [arXiv:hep-ph/0302131].
- [16] K. N. Abazajian, Astropart. Phys. **19**, 303 (2003) [arXiv:astro-ph/0205238].
- [17] A. A. Aguilar-Arevalo *et al.* [The MiniBooNE Collaboration], arXiv:0704.1500 [hep-ex].
- [18] M. Maltoni and T. Schwetz, arXiv:0705.0107 [hep-ph].



- [19] M. Kawasaki, K. Kohri and N. Sugiyama, Phys. Rev. Lett. **82**, 4168 (1999) [arXiv:astro-ph/9811437].  
M. Kawasaki, K. Kohri and N. Sugiyama, Phys. Rev. D **62**, 023506 (2000) [arXiv:astro-ph/0002127].  
K. Ichikawa, M. Kawasaki and F. Takahashi, Phys. Rev. D **72**, 043522 (2005) [arXiv:astro-ph/0505395].
- [20] G. F. Giudice, E. W. Kolb and A. Riotto, Phys. Rev. D **64**, 023508 (2001) [arXiv:hep-ph/0005123].
- [21] S. Hannestad, Phys. Rev. D **70**, 043506 (2004) [arXiv:astro-ph/0403291].
- [22] G. Gelmini, S. Palomares-Ruiz and S. Pascoli, Phys. Rev. Lett. **93**, 081302 (2004) [arXiv:astro-ph/0403323].
- [23] M. Cirelli, G. Marandella, A. Strumia and F. Vissani, Nucl. Phys. B **708**, 215 (2005) [arXiv:hep-ph/0403158].
- [24] K. Abazajian, Phys. Rev. D **73**, 063506 (2006) [arXiv:astro-ph/0511630].
- [25] M. Shaposhnikov and I. Tkachev, Phys. Lett. B **639**, 414 (2006) [arXiv:hep-ph/0604236].